Article

Not peer-reviewed version

Morphological Assessment of Stage HH38 of the Japanese Quail (*Coturnix japonica*) Heart by Micro-Sonogram

Jaden Roe , Ashlyn Benavides , Michael B. Filla , Douglas C. Bittel * , Geetha Haligheri , James E. O'Brien Jr , Nataliya Kibiryeva *

Posted Date: 19 February 2026

doi: 10.20944/preprints202602.1328.v1

Keywords:

echocardiography; cardiovascular embryogenesis; quail (*Coturnix japonica*); doppler

 doi:10.20944/preprints202602.1328.v1

Article

Morphological Assessment of Stage HH38 of the Japanese Quail (*Coturnix japonica*) Heart by Micro-Sonogram

Jaden Roe [1], Ashlyn Benavides [1], Michael B. Filla [1], Douglas C. Bittel [1,*], Geetha Haligheri [2], James E. O'Brien Jr [2] and Nataliya Kibiryeva [1,*]

[1] Kansas City University, Kansas City, MO, USA

[2] Ward Family Heart Center, Children's Mercy Hospital, Kansas City, MO, USA

* Correspondence: nkibiryeva@kansascity.edu

Abstract

A challenge of studying mammalian cardiac embryogenesis is the limited ability to perform experimental manipulations in animal models. The avian embryo is widely accepted as a model for mammalian heart developmental studies. In this study, we establish the methodology and protocols for studying the Japanese quail (*Coturnix japonica*) heart at embryonic day 10 (HH38) using the FUJIFILM VisualSonics Vevo 3100 ultrasound system equipped with a MX550D small animal cardiology transducer. These protocols were designed to measure right ventricular wall thickness, pulmonary artery diameter, and the outflow velocities of the right ventricular outflow tract (RVOT) and the pulmonary artery (PA), thereby establishing baseline parameters of the normally developing quail morphology. Quail embryos are an ideal model for cardiovascular research due to their short incubation period (16-17 days), experimental accessibility, and strong similarities to mammalian heart development. These developmental similarities include, but are not limited to, looping, chamber septation, and the development of a true four-chamber heart. High-resolution imaging modalities, including ultrasound and optical coherence tomography, enable noninvasive, real-time visualization of cardiac morphology and function throughout development. Echocardiography allows for quantitative and qualitative assessments of myocardial structure and cardiac hemodynamics. The similarity to the mammalian heart, combined with rapid embryogenesis, makes quail embryos a valuable model for investigating congenital heart defects, genetic modifications, and fundamental cardiac developmental processes. In this study, we describe reproducible incubation protocols and baseline echocardiographic parameters used to evaluate morphological and physiological changes in the developing embryonic quail heart on embryonic day 10.

Keywords: echocardiography; cardiovascular embryogenesis; quail (*Coturnix japonica*); doppler

1. Introduction

Congenital heart defects are the most prevalent birth defects, affecting approximately 1% of all newborns according to the Centers for Disease Control and Prevention [1,2], and they remain the leading cause of birth defect-associated infant morbidity and mortality [3]. The primary focus of our laboratory is congenital heart defects, with particular emphasis on Tetralogy of Fallot as it is the most common cyanotic congenital heart defect, affecting 5-7% of all congenital heart defects [4]. Tetralogy of Fallot consists of four components: a ventricular septal defect (VSD), overriding aorta, right ventricular outflow tract obstruction (RVOTO), and right ventricular hypertrophy (RVH) [5].

Despite its clinical significance, the precise etiology of Tetralogy of Fallot remains poorly understood. Although several cardiac developmental mechanisms have been proposed, investigation of cardiac malformations in mammalian models is hindered by long gestational periods, regulatory constraints, and substantial financial and logistical burdens associated with mammalian embryonic

 doi:10.20944/preprints202602.1328.v1

research. The establishment of quail as a viable animal model through the production of a baseline morphological parameter set using echocardiography lays the foundation for future comparative studies. One of the proposed mechanisms of Tetralogy of Fallot is through spliceosomal dysregulation. Through genetic modification of various spliceosomal regulatory proteins, it may be possible to reproduce morphologic defects, such as right ventricular hypertrophy, in the developing quail heart in the future. The morphological values, obtained with ultrasound, in these genetically altered quail embryos can then be compared to the normally developed morphological parameter set established in this research. This comparison may lead to the association between these regulatory mechanisms and the etiology of Tetralogy of Fallot.

To address these challenges, we propose the Japanese quail (*Coturnix japonica*) as an effective alternative model for the investigation of cardiovascular developmental patterns. Quail embryos offer several advantages for cardiac developmental research. Most notably, quail heart organogenesis follows a similar embryonic pattern to that of the mammalian heart, including the formation of a true four-chambered heart. Additionally, the quail heart is readily accessible for echocardiographic visualization. Embryonic development is rapid, with a total incubation period of 16-17 days, and a distinct four-chamber anatomy evident by embryonic day 9 or 10. The accessibility, low cost, and short developmental timeline of the quail model enable efficient, large-scale analysis of cardiac morphogenesis [6,7].

Echocardiography was selected as the primary imaging modality due to its noninvasive nature, translational relevance, and clinical applicability, as Tetralogy of Fallot is predominantly diagnosed prenatally using in vivo echocardiography [5]. Using the Fujifilm VisualSonics Vevo 3100 ultrasound system, we performed real-time echocardiographic imaging of the quail heart on embryonic day 10 (HH38). Embryonic day 10 was chosen because it is the last and the largest stage that can be imaged using micro-sonography due to the onset of feathers beyond this stage. It also allows full visualization of the developed four-chamber heart. Two-dimensional measurements and Doppler assessments were used to quantify cardiac outflow velocities, ventricular wall thickness, and pulmonary arterial diameter. Many scans were performed, the majority of which served to train our team and to allow them to determine what protocols should be followed for producing quality scans. The scans with the best visualization were then analyzed to establish the baseline morphological and functional parameters of the normally developing quail heart. These data points will serve as a reference framework for future comparative studies, including genetic knockdown studies investigating the developmental origins of congenital heart defects. The goal is that these structural changes could be compared to a human fetus, as the underlying defect is the same.

2. Methods and Procedures

All procedures were conducted in accordance with institutional guidelines for the care and use of avian embryos.

2.1. Procurement and Incubation of Quail Eggs

Fertilized quail eggs were purchased from Ozark Egg Company, Stover MO. Early incubation efforts targeted approximately 40 eggs per cohort to support imaging throughput with an expected incubation success rate of 70%. Subsequently, a twice-weekly incubation schedule was adopted, with 20 eggs set for incubation on Mondays and Tuesdays to allow for completion of incubation on the following Thursday and Friday, corresponding to 10 days of embryonic development.

The incubation period of 10 days was selected due to developmental constraints associated with quail embryogenesis. Japanese quail begin feather development at approximately embryonic day 9, with substantial feather growth continuing after day 10 [8]. During experimentation, we observed that feather formation significantly impairs echocardiographic visualization of the developing heart by introducing artifacts and acoustic shadowing, thereby reducing image quality and data reliability.

To control for confounding variables, the fertilized eggs were homogeneously distributed on an incubation tray in a Genesis model 1588 Hova-Bator Incubator, Savannah, GA maintained at 38 °C.

 doi:10.20944/preprints202602.1328.v1

Each egg was marked on the superior surface to ensure consistent orientation during post-incubation access. Throughout the incubation period, distilled deionized water was added to the chamber's reservoir to maintain appropriate humidity levels for proper growth conditions.

2.2. Quail Embryo Preparation for Echocardiography

Japanese quail (*Coturnix japonica*) are a well-established avian model for chorioallantoic membrane (CAM)-based research [9]. The CAM permits direct visualization of the developing embryo, while maintaining intact vascular structures, thereby preventing exsanguination during imaging. This feature of the quail model enables prolonged visualization and repeated echocardiographic assessment of the embryonic heart.

Preparation of the quail embryos for echocardiography required careful temperature control throughout the procedure to preserve embryonic viability throughout the procedure. Although embryos were humanely terminated in accordance with institutional and regulatory guidelines following imaging, it was essential to maintain normothermic incubation-like temperatures during preparation and scanning. To achieve this, several procedures were performed as follows. Eggs not actively being prepared or scanned were kept in the incubator until use. Upon removal for shell preparation, eggs were immediately placed on a heating pad. During echocardiographic imaging, temperature was maintained by circulating warm air through a custom 3D-printed imaging incubator which supported the egg in an aluminum foil cradle with heated airflow beneath it by the Airtherm SMT Model 98736-3 heater from World Precision Instruments (Figure 1).

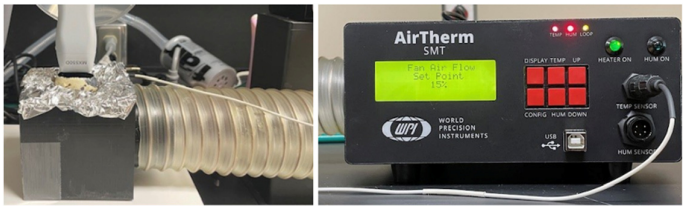

Figure 1. 3D-printed imaging incubator with warm air circulated underneath.

Egg shell removal was performed on a heated surface under direct illumination to enhance visualization (Figure 2). A molded aluminum foil support was used to stabilize the egg and prevent its rolling during manipulation. The peeling process was initiated by gently tapping the inferomedial aspect of the egg with the blunt end of a dull instrument, just below the reference line on the superior aspect of the egg marked during incubation. This initial opening facilitated a controlled shell removal process using forceps. Care was taken to avoid damaging the thick outer membrane beneath the shell, which is adherent to the underlying chorioallantoic membrane containing the embryo's vasculature, to prevent rupture of these vessels and resultant exsanguination. A visualization window approximately 3 cm x 2 cm, making up most of the superior aspect of the egg, was created. The outer membrane was then carefully separated from the chorioallantoic membrane, as disruption of the latter results in rapid exsanguination and significantly diminishes the duration of viable imaging. Small tears in the outer membrane were used as initiation points to facilitate this controlled separation process.

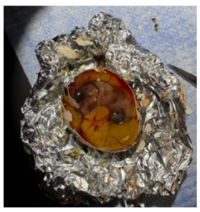

Figure 2. Quail shell removal set-up with quail egg placed in an aluminum foil cradle, with a heating pad underneath, and a light aimed directly on the superior aspect of the egg.

 doi:10.20944/preprints202602.1328.v1

Following shell and membrane removal, the egg was prepared and positioned for echocardiographic imaging. A double-layered aluminum foil insert was secured within the 3D-printed incubator, and the prepared egg was positioned upon this heated opening. A square sheet of clingwrap was placed tautly over the visualization window to form a stable imaging interface for the echo probe. Gauze was placed between the foil borders and the positioned egg to further stabilize the egg and prevent its shifting during scanning. Throughout imaging, 38 °C air was continuously circulated beneath the foil cradle to maintain appropriate temperature conditions.

2.3. Echocardiographic Imaging of Quail Embryos

To begin, a small amount of ultrasound gel, the size of a quarter, was applied to the clingwrap covering each egg and evenly distributed using the echo probe to ensure proper acoustic coupling. Multiple scans were performed on each embryo to obtain consistent morphological and functional data.

Scans were acquired in both long-axis and short-axis views. The long-axis view provided detailed visualization of cardiac morphology, allowing measurement of myocardial thickness, right ventricular outflow tract and pulmonary outflow velocities, and pulmonary arterial diameter. The short-axis view allowed for additional measurement of the myocardial thickness, as well as primary measurement of right ventricular outflow tract velocity. Attempts to utilize the M-Mode function of the Vevo 3100 system were unsuccessful. M-Mode is universally utilized to quantify cardiac function. However, the size of the quail embryologic heart and the rapid heart rate limited the reproducibility of this parameter. Future work will seek to incorporate this imaging modality and standardize its implementation.

The process of scanning was initiated by lowering the echo probe gently onto the embryo's surface to calibrate the image on the Vevo 3100 system. Further manipulation was needed to obtain the long-axis view, which served as an anchor image for the rest of the scanning process. At the long-axis view, a B-Mode scan was performed to visualize all the relevant anatomical structures, such as the cardiac chambers and outflow tracts. The probe was then adjusted to prioritize visualization of the ventricular wall to measure the ventricular outflow dimensions, followed by Doppler. However, the visualization of the ventricular outflow in the long-axis was sometimes inconsistent. The probe was further manipulated cranially along this same axis to visualize the pulmonary artery, allowing B-Mode measurement of diameter and Doppler assessment of outflow velocity.

Rotation of the echo probe 90° from the long-axis view provided the short-axis view. From this view, fine adjustments were required to frame the heart properly. Following visualization of this view, both B-Mode and Doppler scans were obtained to provide analysis for ventricular wall thickness and ventricular outflow tract velocity, respectively. The Doppler probe on the Vevo 3100 screen was localized to the right ventricle for outflow tract velocity measurement during scanning. All aforementioned processes and steps were performed on every viable embryo.

Due to the small size of the quail embryos, with structures often less than 0.5 mm thick, precise echo probe manipulation was critical. To improve operator skill and efficiency, 2-4 chicken embryos were incubated and scanned as practice models alongside the quail embryos but were not utilized for data collection. Familiarity with human echocardiographic procedures also facilitated efficient imaging on the Vevo 3100 system due to the inherent ability to not have to reposition the probe for every scan.

2.4. Quantification of Embryonic Cardiac Morphology and Function

For each morphological feature, the 10 highest-quality B-Mode scans were selected for analysis. Right ventricular wall thickness was measured 10 times per scan across the wall's entirety, from one hyperechoic edge to the opposing hyperechoic edge, in both systole and diastole. The 10 measurements from each scan were averaged to yield a single data point per scan, and the 10 resulting scan averages were further averaged to obtain a final mean value. Because right ventricular wall thickness was visualized in both long- and short-axes, this process was performed in the long-

 doi:10.20944/preprints202602.1328.v1

axis and repeated upon manipulation to the short-axis. Pulmonary artery thickness was measured using the same procedure in the long-axis view only.

For outflow velocities, the 10 best Doppler scans were selected for analysis. Pulmonary artery outflow velocity was measured distal to the right ventricle in the long-axis view, whereas right ventricular outflow tract velocity was measured in the center of the right ventricular chamber in the short-axis view. These 10 scans were then averaged to give a single data point for the mean outflow velocity.

For all assessments, mean values were calculated along with standard deviation, range, and median to provide a comprehensive summary of the measurements.

3. Results

3.1. Echocardiographic Visualization of the Embryonic Quail Heart

High-resolution echocardiographic imaging enabled consistent visualization of the embryonic quail heart at embryonic day 10. Both long-axis and short-axis views were successfully acquired, allowing visualization of the right ventricular wall, pulmonary artery, and associated outflows. Representative B-Mode and Doppler images of various scans are presented in Figure 3.

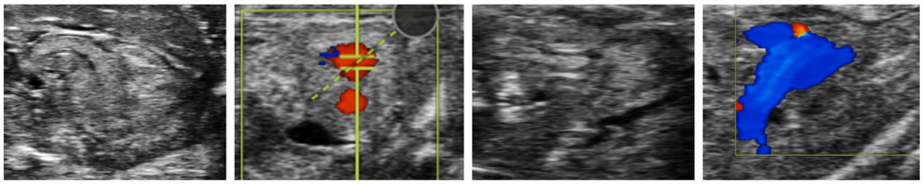

Figure 3. From left to right: (1- long-axis B-Mode localized at ventricles, 2- short-axis Doppler of the right ventricle outflow tract, 3- long-axis B-Mode localized at the pulmonary artery, 4- long-axis Doppler of the pulmonary artery outflow tract).

3.2. Long-Axis Right Ventricular Wall Thickness

Right ventricular wall thickness was measured in both long- and short-axis views. In the long-axis view, right ventricular wall thickness averaged 0.429 ± 0.049 mm in systole and 0.428 ± 0.049 mm in diastole. Representative systolic and diastolic long-axis images are presented in Figure 4. Summary statistics for long-axis right ventricular wall thickness are provided in Table 1.

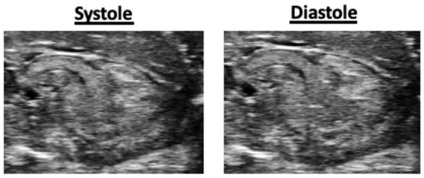

Figure 4. Systolic and diastolic long-axis B-Mode scans of right ventricular wall thickness.

Table 1. Long-axis right ventricular wall thickness measurements summary.

	Systolic (mm)	Diastolic (mm)
Mean	0.4293083	0.42823602
Standard Deviation	0.048913834	0.048913834
Range	(0.308208,0.560907)	(0.329723,0.551333)
Median	0.425528	0.4258585

 doi:10.20944/preprints202602.1328.v1

3.3. Short-Axis Right Ventricular Wall Thickness

In the short-axis view, right ventricular wall thickness averaged 0.462 ± 0.074 mm in systole and 0.452 ± 0.070 mm in diastole. Representative systolic and diastolic short-axis images are presented in Figure 5. Summary statistics for short-axis right ventricular wall thickness are provided in Table 2.

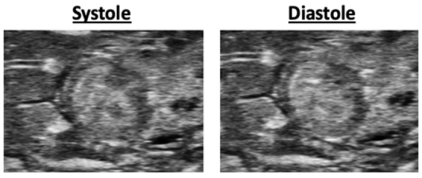

Figure 5. Systolic and diastolic short-axis B-Mode scans of right ventricular wall thickness.

Table 2. Short-axis right ventricular wall thickness measurements summary.

	Systolic (mm)	Diastolic (mm)
Mean	0.461885	0.451995
Standard Deviation	0.074358	0.070346
Range	(0.317666, 0.689367)	(0.308807, 0.62099)
Median	0.458301	0.449253

3.4. Pulmonary Artery Diameter

Pulmonary artery diameter was measured in the long-axis view. The pulmonary artery diameter averaged 0.320 ± 0.067 mm in systole and 0.292 ± 0.043 mm in diastole. Representative systolic and diastolic images are presented in Figure 6. Summary statistics for pulmonary artery diameter are provided in Table 3.

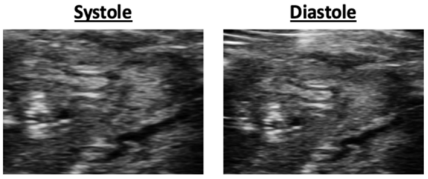

Figure 6. Systolic and diastolic long-axis B-Mode scans of pulmonary artery diameter.

Table 3. Long-axis pulmonary artery measurements summary.

	Systolic (mm)	Diastolic (mm)
Mean	0.319532	0.292096
Standard Deviation	0.066594	0.042508
Range	(0.172243, 0.46589)	(0.181652, 0.396769)
Median	0.310706	0.294285

3.5. Right Ventricular Outflow Velocity

Right ventricular outflow velocity was measured in the short-axis view. The right ventricular outflow velocity averaged 177.922 ± 16.48 mm/s. Although Doppler was used to obtain this measurement, the respective Doppler and B-Mode imaging are presented in Figure 7. Summary statistics for right ventricular outflow velocity are provided in Table 4.

 doi:10.20944/preprints202602.1328.v1

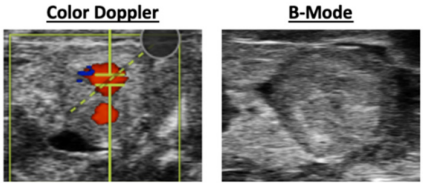

Figure 7. Color Doppler and B-Mode scans of right ventricular outflow tract velocity.

Table 4. Doppler right ventricular outflow tract velocity measurements summary.

Right Ventricle Outflow Velocity	**(mm/s)**
Mean	177.9219
Standard Deviation	16.47633
Range	(145.8112, 218.5378)
Median	175.4263

3.6. Pulmonary Artery Velocity

Pulmonary artery velocity was measured in the long-axis view. The pulmonary artery velocity averaged 132.136 ± 20.66 mm/s. The respective Doppler and B-Mode imaging are presented in Figure 8. Summary statistics for pulmonary artery velocity are provided in Table 5.

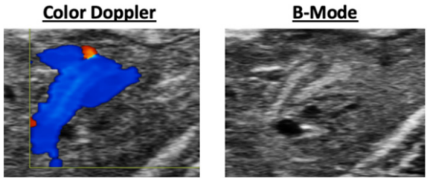

Figure 8. Color Doppler and B-Mode scans of pulmonary artery velocity.

Table 5. Doppler pulmonary artery velocity measurements.

Pulmonary Artery Velocity	**(mm/s)**
Mean	132.1363
Standard Deviation	20.66033
Range	(95.15182, 166.8929)
Median	126.9936

Collectively, these measurements establish baseline morphological and functional parameters of the normally developing embryonic quail heart at embryonic day 10.

4. Discussion

This study establishes the Japanese quail (Coturnix japonica) as a viable animal model for the echocardiographic assessment of embryonic cardiac morphology and function. Utilizing high-resolution ultrasound imaging, we successfully obtained reproducible long- and short-axis views of the quail embryo heart at embryonic day 10. We also quantified significant structural and hemodynamic parameters, including right ventricular wall thickness, pulmonary artery diameter, and cardiac outflow velocities. Collectively, these measurements provide a substantial baseline framework for the normally developing quail heart.

Notably, avian species, including quail, have been reported to exhibit a higher incidence of sporadic congenital heart defects compared to humans. This characteristic further strengthens the utility of the quail model for investigating the etiology of these defects, particularly Tetralogy of Fallot. In this study, consultation with a pediatric cardiologist allowed for the identification of echocardiographic features that were suggestive of structural defects within several scans. Although

 doi:10.20944/preprints202602.1328.v1

systematic classifications of congenital heart defects are beyond this work, these observations highlight the feasibility of detecting and characterizing congenital defects in the developing quail embryo utilizing our techniques.

In a broad sense, the objective of this research is to establish a comparable morphological parameter set to support future studies investigating the molecular regulation of cardiogenesis. Our laboratory focuses on the function of the spliceosomal apparatus, and the role it plays in organogenesis of the heart, with particular interest in a subset of small non-coding RNAs known as Small Cajal body-associated RNAs (scaRNAs) and their role in the regulation of this apparatus. Our future studies will utilize targeted genetic knockdown approaches to disrupt specific scaRNAs in the developing quail embryos to ascertain their effect on cardiogenesis. Using the echocardiographic protocol and baseline morphological parameters established here, these future genetically modified embryos will be quantitatively compared to the normally developing controls. Deviations in ventricular wall thickness, vascular dimensions, or flow velocities would support an association between spliceosomal dysregulation and the development of congenital heart defects.

Although this study establishes the first baseline morphological parameter set, it is not without limitations. Measurements were obtained at a single developmental time point, constraining the application to a single point in time. Future studies implementing shell-less (Egg-in-cube) in vitro methods will allow for longitudinal optical coherence tomography and micro-sonogram studies of the same embryo over multiple stages [10]. Longitudinal assessment across multiple embryonic stages will be possible using this in vitro system and will lead to further understanding of these morphological processes by allowing for manipulation and imaging at various stages. Additionally, the utilization of a computer algorithm for measurement of these morphological parameters would help strengthen uniform methodology of data collection. This was not performed due to time restrictions and restrictions of the Vevo 3100 system itself. The function that would have had the highest data yield was M-Mode mapping. This allows for the mapping of the ventricular chamber movement, in the short-axis, to gather data on ejection fraction, wall thickness, etc. During our study, we found it incredibly challenging to gather this data due to the increased hyperechoic presentation in the chamber itself that disrupted the measurement. This could have been due to human error or instrumentation, but the proper use of the M-Mode feature would certainly be worth investigating to gather these measurements. Despite these limitations, the present work still provides a critical methodological and quantitative foundation for future genetic and developmental studies.

In summary, this study demonstrates that high-resolution echocardiography is a viable method for reliable, qualitative assessment of the embryonic cardiac morphology of the Japanese quail. The baseline parameter set established here supports the use of this model for future investigations into the molecular and genetic origins of various congenital heart defects and reveals the developing quail embryo as a powerful model for the investigation of translational cardiovascular research.

Author Contributions: Jaden Roe was the primary investigator that formulated the project methodology off the conceptualization established by other authors. He was responsible for the data curation and formal analysis as well as writing the original draft preparation, reviewing, and editing the manuscript. Ashlyn Benavides was a primary investigator that was responsible for carrying out methodology and data curation. She also contributed to discussion on congenital heart defects and reviewing and editing the manuscript. Dr. Geetha Haligheri, a pediatric cardiologist, participated as the physician who aided in formalizing clinical hypothesis, performance of the imaging, as well as reviewing the images obtained for validation and interpretation. She was actively involved in editing the manuscript relating to congenital heart disease and imaging aspects. Michael B. Filla conceptualized the incubator system with egg-in-cube culture in mind and adapted it for use in the opened eggshell model for collecting baseline control statistics. Demonstrated techniques to increase embryo viability. Contributed revisions and proper usage of avian embryo nomenclature and significance to mammalian heart where appropriate to the original draft. Drs. James O'Brien and Douglas C. Bittel were involved in establishing and designing the project, reviewing the data, and revising the manuscript. Dr. Nataliya Kibiryeva was involved

 doi:10.20944/preprints202602.1328.v1

in the conceptualization, establishment, design, and supervision of the project. As well as reviewing the data and the manuscript. All authors have read and agreed to the published version of the manuscript.

Funding: Funding was obtained from the Kansas City University Intramural Grant Discovery program and the Ward Family Heart Center at Children's Mercy Hospital, Kansas City, Missouri.

Institutional Review Board Statement: The Kansas City University Institutional Review Board has reviewed this project and agreed that it is nonhuman subjects research and is therefore exempt.

Data Availability Statement: Data is included in the manuscript. Raw data can be requested from the corresponding author.

Acknowledgments: This work was supported by the Kansas City University Summer Student Research Fellowship (N.P.), the Kansas City University Intramural Grant Discovery Program (EHS), Victor E. Speas Foundation, and the Ward Family Heart Center at Children's Mercy Hospital.

Conflicts of Interest: The authors declare no conflicts of interest. The funders had no role in the design of the study; in the collection, analyses, or interpretation of data; in the writing of the manuscript; or in the decision to publish the results.

References

1. Hoffman, J.I.E.; Kaplan, S. The incidence of congenital heart disease. *J. Am. Coll. Cardiol.* **2002**, *39*, 1890–1900, doi:10.1016/S0735-1097(02)01886-7.
2. Reller, M.D.; Strickland, M.J.; Riehle-Colarusso, T.; Mahle, W.T.; Correa, A. Prevalence of congenital heart defects in metropolitan Atlanta, 1998–2005. *J. Pediatr.* **2008**, *153*, 807–813, doi:10.1016/j.jpeds.2008.05.059.
3. Oster, M.E.; Lee, K.A.; Honein, M.A.; Riehle-Colarusso, T.; Shin, M.; Correa, A. Temporal trends in survival among infants with critical congenital heart defects. *Pediatrics* **2013**, *131*, e1502–e1508, doi:10.1542/peds.2012-3435.
4. Horenstein, M.S.; Diaz-Frias, J.; Guillaume, M. Tetralogy of Fallot. In *StatPearls* [Internet]; StatPearls Publishing: Treasure Island, FL, USA, 2025 Jan–. Available online: https://www.ncbi.nlm.nih.gov/books/NBK513288/
5. Wilson, R.; Ross, O.; Griksaitis, M.J. Tetralogy of Fallot. *BJA Educ.* **2019**, *19*, 362–369, doi:10.1016/j.bjae.2019.07.003.
6. Lansford, R.; Rugonyi, S. Follow Me! A tale of avian heart development with comparisons to mammal heart development. *J. Cardiovasc. Dev. Dis.* **2020**, *7*, 8, doi:10.3390/jcdd7010008.
7. Wittig, J.G.; Münsterberg, A. The chicken as a model organism to study heart development. *Cold Spring Harb. Perspect. Biol.* **2020**, *12*, a037218, doi:10.1101/cshperspect.a037218.
8. Ainsworth, S.J.; Stanley, R.L.; Evans, D.J.R. Developmental stages of the Japanese quail. *J. Anat.* **2010**, *216*, 3–15, doi:10.1111/j.1469-7580.2009.01173.x.
9. Kundeková, B.; Máčajová, M.; Meta, M.; Čavarga, I.; Bilčík, B. Chorioallantoic membrane models of various avian species: Differences and applications. *Biology* **2021**, *10*, 301, doi:10.3390/biology10040301.
10. Liu, J.; Wang, Z.; Gao, X.; Wang, Q.; Liang, X.; Zhang, H.; Wang, W.; Ji, S. Mechanisms of hemodynamic shear stress in regulating endothelial cell function and vascular diseases. *Front. Physiol.* **2022**, *13*, 893736, doi:10.3389/fphys.2022.893736.